A Journal of the Gesellschaft Deutscher Chemiker
Angewandte Chemie
GDCh
International Edition
www.angewandte.org

Accepted Article

Title: Robust synthesis of Au-based multishell structures as plasmonic catalysts for selective hydrogenation of 4-nitrostyrene

Authors: Shuyan Song, Jian Li, Yu Liu, Lingling Zhang, Qishun Wang, Xiao Wang, Hongjie Zhang, and Yan Long

To be cited as: *Angew. Chem. Int. Ed.* 10.1002/anie.201910836
Angew. Chem. 10.1002/ange.201910836

Link to VoR: http://dx.doi.org/10.1002/anie.201910836
http://dx.doi.org/10.1002/ange.201910836

WILEY-VCH

Robust synthesis of Au-based multishell structures as plasmonic catalysts for selective hydrogenation of 4-nitrostyrene

Jian Li,[a,b] Yan Long,[a] Yu Liu,[a] Lingling Zhang,[a] Qishun Wang,[a,b] Xiao Wang,[a] Shuyan Song,*[a,b] and Hongjie Zhang[a,b]

Abstract: In this paper, we describe a robust self-template strategy for facile and large-scale synthesis of porous multishell Au with controllable shell number, sphere size and in-situ surface modification. The process involved the rapid reduction of novel Au-melamine colloidal templates with a great amount of $NaBH_4$ in presence of poly(sodium-p-styrenesulfonate) (PSS). After soaking the templates in other metal salt solution, the obtained bimetallic templates could also be generally converted into bimetallic multishell structures by same reduction process. In the hydrogenation of 4-nitrostyrene using NH_3BH_3 as a reducing agent, the porous triple-shell Au with surface modification (S-PTSAu) exhibited excellent selectivity (97 %) for 4-aminostyrene in contrast with unmodified triple-shell Au. Furthermore, it also showed higher enhancement of catalytic activity under irradiation of visible light as compared to similar catalysts with less shell number. This work opens up a new route in designing and synthesizing Au-based multishell structures for various applications.

*F*abricating metal catalysts with attractive structure and excellent performance have received much attention in recent years.[1-3] To evaluate their performance, the catalytic selectivity plays an important role for specific organic reaction. Chemical modification is one of effective strategy for tuning electronic states and steric environment of metal catalysts and further improving their selectivity.[4,5] However, the greatly reduced activity was also observed in these modified catalysts due to the influence of modifier.[6,7] Plasmonic catalysis has emerged as effective routes to accelerate chemical reactions under mild and environmentally friendly conditions.[8,9] As one of excellent plasmonic catalysts, Au materials can not only catalyze a series of organic reactions, but also harvest and utilize visible light energy to promote these reactions.[8,9] Constructing multishell structures of Au may further increase their plasmonic catalytic activity, since the porous multiple shells can provide larger specific surface area, enable molecules to access to the interior of structures and increase light-harvesting.[10-11]

For the synthesis of multishell noble metal, current methods have mainly focused on the use of galvanic replacement reactions, involving multiple growing and etching of sacrificial shells.[12,13] These preparation procedures are tedious, especially for shell number above two, and the obtained products show low reproducibility, which hinders their further applications. Interestingly, multishell structure of metal oxide can be facile formation by controlling decomposition of metal-organic template.[14,15] However, successful examples in noble metal have yet to be reported,[16,17] largely due to the lack of suitable template and the corresponding conversion strategy. On one hand, there are limited reports about metal-organic colloidal particles of noble metal, especially containing Au ions.[18,19] On the other hand, unlike metal oxide clusters, the Au clusters generated by the decomposition of a template can rapidly aggregate and regrow into bulk materials owing to their high surface free energies,[20] which would increase difficulty in controlling morphology.

Herein, we synthesized novel Au-melamine colloidal spheres by directly heating aqueous solution of Au^{3+} and melamine at 70 ºC. By rapidly adding a great amount of $NaBH_4$ into mixed solution containing colloidal sphere and PSS, the multishell Au with in-stiu modification of reducing PSS could be obtained. The scanning electron microscopy (SEM) images (Figure 1a and b) and the transmission electron microscopy (TEM) images (Figure 1c) reveal that the solid template spheres with average diameters of 400 nm (Figure S1a) possess uniform structure and smooth surfaces. The X-ray powder diffraction (XRD) pattern (Figure S1b) and the high-resolution X-ray photoelectron spectroscopy (XPS) spectrum (Figure S1c) of Au display the

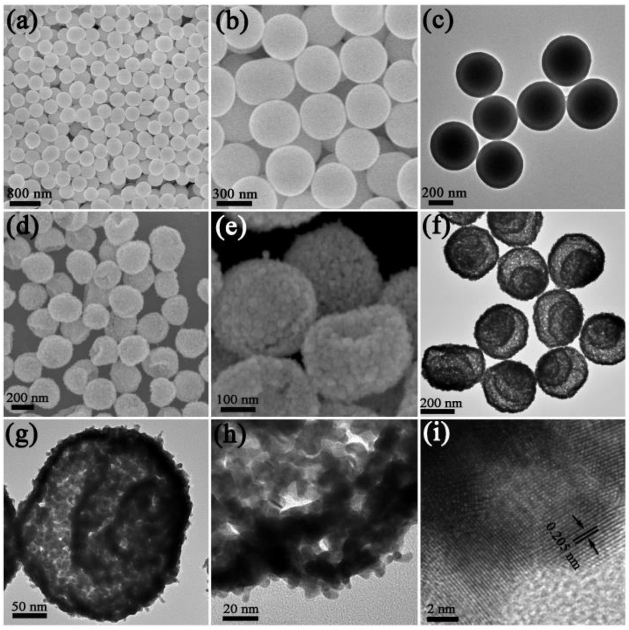

Figure 1. (a-b) SEM images with different magnification, (c) TEM images for Au-melamine spheres; (d-e) SEM images, (f-h) TEM images with different magnification, and (i) HRTEM image of S-PTSAu.

---

[a] J. Li, Y. Long, Y. Liu, L. L. Zhang, Q. S. Wang, Dr. X. Wang, Prof. S. Y. Song, and Prof. H. J. Zhang
State Key Laboratory of Rare Earth Resource Utilization,
Changchun Institute of Applied Chemistry, Chinese Academy of Sciences, Changchun 130022, P. R. China.
E-mail: songsy@ciac.ac.cn
[b] J. Li, Q. S. Wang, Prof. S. Y. Song, and Prof. H. J. Zhang
School of Applied Chemistry and Engineering, University of Science and Technology of China, Hefei 230026, Anhui, P. R. China.

Supporting information for this article is given via a link at the end of the document.

10.1002/anie.201910836

formation of amorphous colloidal sphere containing Au^{3+}. The Fourier transform infrared (FT-IR) spectra (Figure S1f) show that the colloidal sphere might be formed by complicated hydrogen-bond interaction. The colloidal sphere with average size of 400 nm can be adjusted to 254 nm and 130 nm by changing experiment conditions (Figure S2). Unlike templates, the reduced samples illustrate vesicle-like morphology with rough surfaces and decreased average diameter of 288 nm (Figure 1d, e and S3a). The TEM images (Figure 1f, g and S3b) reveal that the spheres possess a clear triple-shell structure. These porous shells consist of Au branches, which are formed by mutual fusion of small Au nanoparticles. A large number of interstices between branches with size below to 10 nm are distributed throughout the shells (Figure 1h). The high resolution TEM (HRTEM) image illustrates that the lattice distances are 0.205 nm (Figure 1i), corresponding to the (200) planes of metal Au.

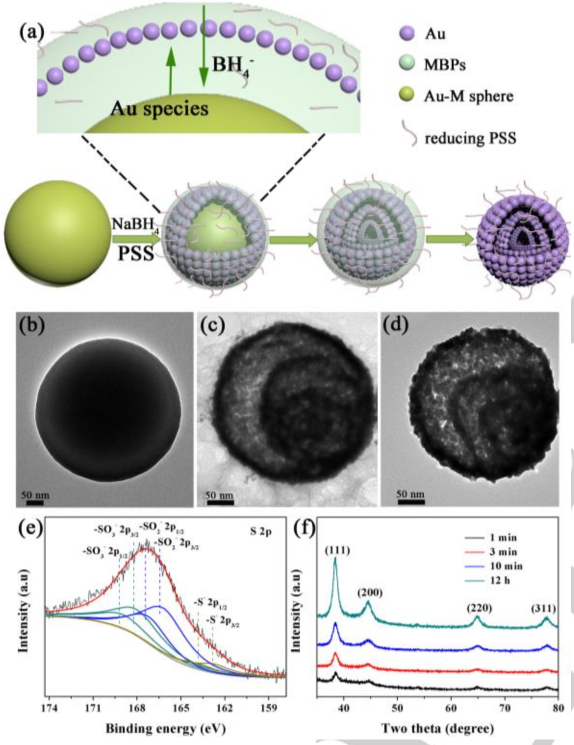

Figure 2. (a) Schematic. (b) TEM image of Au-melamine sphere. (c) TEM image of triple shell Au after reaction for one minute without the addition of PSS. (d) TEM image of S-PTSAu, (e) XPS spectrum of S 2p for S-PTSAu. (f) XRD patterns of S-PTSAu after reaction for different time.

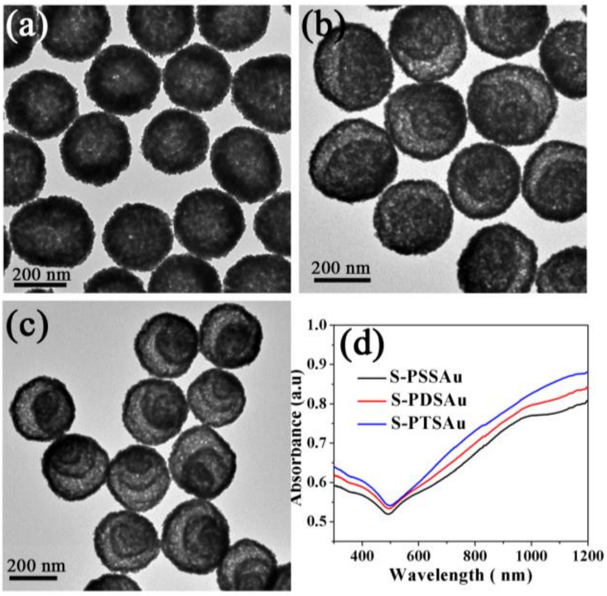

Figure 3. TEM images of (a) S-PSSAu, (b) S-PDSAu and (c) S-PTSAu. (d) UV-Vis-NIR absorption spectra of different samples with same Au concentration (90 ppm).

In order to weaken the diffusion and growth of small Au nanoparticles, the mixed solvents of water and ethylene glycol with high viscosity were used in reduction process (Figure S4). If no PSS was added in reactions, the only aggregated multishell Au spheres were obtained (Figure S5a-b). The TEM images of sample after reaction for one minute show that the completed multishell structures already form at this time (Figure 2c and S6a). However, the whole sphere is covered by the residual melamine-based polymers (MBPs) (Figure 2c and S6). Most of MBPs would separate from the Au surfaces with further reaction (Figure S5). Because the reduction rate of colloidal sphere is faster than separation rate of MBPs, the formation of multishell Au is limited within the MBPs, which not only weakens the uncontrollable regrowth of small Au nanoparticles but also prevents their departure to form free nanoparticles. Therefore, the relatively slow separation of MBPs effectively assists the formation of completed multishell structures. The addition of PSS to original solution can obtain the dispersive samples. The XPS spectrum of S 2p (Figure 2e) shows presence of three types of sulfur species in final sample, including sulfonate ($–SO_3^-$), sulfinate ($–SO_2^-$) and the sulfide ($-S^-$). These results display that part of $–SO_3^-$ in PSS is reduced into $–SO_2^-$ and $-S^-$ by highly active hydrogen in $NaBH_4$ to form reducing PSS, which is similar to the formation of S^{2-} and S_2^{2-} from SO_3^{2-}.[21] These reducing PSS with a stronger coordinated capability will stabilize the Au sphere to form S-PTSAu. Additionally, XRD patterns (Figure 2f) of samples reacting for different time and the TEM images in Figure S7 indicate that the initial reduction stage can obtain MBPs-protected shells consisting of small Au nanoparticles. Along with gradual separation of MBPs, these small Au nanoparticles will regrow via mutual fusion process, finally leading to form porous shells. The more detailed formation process can be found in supporting information.

Furthermore, we discovered that changing reaction temperature could effectively tune shell numbers. For example, the single, double and triple-shell Au with surface modification (S-PSSAu, S-PDSAu and S-PTSAu) formed at the temperature of 0 °C, 10 °C and 25 °C, respectively (Figure 3a-c). It is postulated that increased reaction temperature can decrease viscosity of solvent and greatly accelerate BH_4^- to diffuse into the interior of colloidal sphere (Figure 2a). As a result, the inward diffusion of BH_4^- is much faster than outward diffusion of Au species. These diffusion rate distinctions finally lead to formation of multishell structures.[22-24] UV–Vis–NIR spectra (Figure 3d) of three samples (S-PSSAu, S-PDSAu and S-PTSAu) with same Au concentration were determined to investigate their

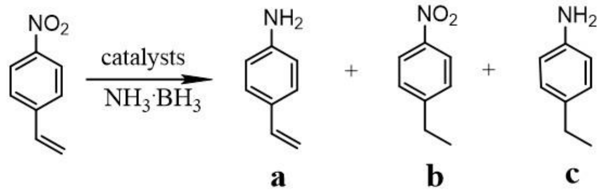

		light				dark			
			selectivity/%				selectivity/%		
entry	catalysts	conversion/%	a	b	c	conversion/%	a	b	c
1	PTSAu/ZrO$_2$	>99	77	0	23	>99	84	0	16
2	S-PTSAu	>99	97	0	3	14	96	1	3
3	S-PDSAu	84	97	0	3	13	95	1	4
4	S-PSSAu	65	95	1	4	11	96	1	3

Table 1. Selective Hydrogenation of 4-nitrostyrene over PTSAu/ZrO$_2$, S-PTSAu, S-PDSAu and S-PSSAu under Visible Light Irradiation and in the Dark. Experiment conditions: 4-nitrostyrene (0.2 mmol), $NH_3{\cdot}BH_3$ (0.5 mmol), Au (1.5 mol%), Xe lamp at 0.5 W·cm^{-2} with 420 nm cutoff filter at 298 K. The reaction time is 2 h.

light absorption property. Accompanied by the increasing shell number, increased light-harvesting is observed, which may be caused by the presence of additional incident light reflections in the structures with more shells.[10,11] Moreover, converting 254 nm and 130 nm colloidal spheres can obtain 160 nm and 90 nm (Figure S8) Au spheres, respectively. Because of the robust conversion process, these multishell Au spheres could be easily synthesized by expanding the synthetic scale by a factor of 20, and the samples still maintained high quality (Figure S9). More importantly, such a simple strategy is also suitable for generally fabricating Au-based bimetallic multishell structures. For example, the Au-Ag, Au-Cu and Au-Pt multishell structures were synthesized by soaking the templates in corresponding salt solution and further reducing the obtained templates (Figure S10).

Selective reduction of Ar-NO$_2$ in the presence of Ar-C=C can lead to the formation of functional amines, which are important industrial intermediates for pharmaceuticals, fine chemicals, and polymers.[25,26] NH_3BH_3 with advantages of high hydrogen storage capacity and long-term stability is a new candidate as a hydrogen donor for hydrogenation reactions.[27] We chose the hydrogenation of 4-nitrostyrene as the probe reaction to investigate the influence of surface modification and multishell structure on catalytic performance of Au sphere. The catalytic reaction was implemented using NH_3BH_3 as a reducing agent. The ZrO$_2$ supported triple-shell Au (PTSAu/ZrO$_2$) as unmodified contrast sample was also synthesized without addition of PSS (Figure S11a). Catalytic results under visible light irradiation and in the dark are provided for comparison. As shown in Table 1 (entry 1), the PTSAu/ZrO$_2$ showed >99 % conversion in both light and dark conditions. However, their poor selectivity of 4-aminostyrene (77 % in the light and 84 % in the dark) were also observed. In contrast, the S-PTSAu displayed only 14 % conversion in the dark, but >99 % conversion in visible light irradiation. At the same time, it also possessed 97 % of selectivity for 4-aminostyrene (Table 1, entry 2). Their selectivity could maintain at 97 %, even though the reaction time was prolonged to 12 h. The influence of ZrO$_2$ can be ignored, since the selectivity of ZrO$_2$ supported S-PTSAu is the same as S-PTSAu. We further tested time profiles of both modified and unmodified sample. The time profiles of PTSAu/ZrO$_2$ (Figure S12a) displayed rapid reduction of –NO$_2$, and slow overhydrogenation could also be observed. For S-PTSAu/ZrO$_2$, the catalytic activity was greatly weakened (Figure S12b), which is not surprising as the poison ability of sulfhydryl group in reducing PSS.[4,32] More importantly, the overhydrogenation reaction was prevented in S-PTSAu/ZrO$_2$ system (Figure S12b). The $NH_3{\cdot}BH_3$-initiated hydrogenation of a mixture of nitrobenzene and styrene was further tested using two catalysts. The results (Table S1) show that PTSAu/ZrO$_2$ are active towards reduction of Ar-NO$_2$ and Ar-C=C, while the S-PTSAu/ZrO$_2$ activate only Ar-NO$_2$, not Ar-C=C. The transfer hydrogenation processes have been proposed in AB-initiated hydrogenation reactions.[28-30] In these processes, the polarized hydrogen atom in $NH_3{\cdot}BH_3$ would transfer to unsaturated groups.[28-31] The modification of sulfhydryl species on Au surface might influence polarized hydrogen transfer towards -C=C, finally resulting in their high selectivity. The unmodified Au/ZrO$_2$ was also synthesized (Figure S11c) by simple reduction of HAuCl$_4$ and ZrO$_2$ nanoparticles mixture solution with NaBH$_4$. In order to confirm the influence of sulfhydryl species modification, the Au/ZrO$_2$ was further treated with L-cystine to obtain modified sample (S-Au/ZrO$_2$). The catalytic results (Table S2) show that selectivity (96 %) of S-Au/ZrO$_2$ is obviously higher than Au/ZrO$_2$ (71 %).

The catalytic results of entries 2-4 in Table 1 indicate that Au spheres with more shell number exhibit obvious higher photocatalytic activity. Specifically, the conversion (> 99 %) of S-PTSAu in same light conditions was higher than those of S-PDSAu (84 %) and S-PSSAu (65 %). When reactions are implemented under irradiation of visible light, S-PTSAu can absorb light energy by localized surface plasmon resonance

(LSPR) [33, 34] and further generate massive hot electrons on the Au surfaces via the surface plasmon decay process.[2, 35] These hot electrons will promote dissociation of absorbed NH_3BH_3 and further reduce the adjacent $-NO_2$ group, finally resulting in improvement of hydrogenation activity.[2, 35] The highest photocatalytic activity of S-PTSAu in entries 2-4 might be mainly attributed to that porous triple-shell structures provide more of active sites and promote light-harvesting (Figure 3d). At the same time, the more of plasmonic coupling between shells in triple-shell structures might also contribute to their higher photocatalytic activity.[35-36] Additionally, these surface-modified samples also display excellent durability in reactions. As shown in Figure S13a, S-PTSAu still exhibited similar activity and selectivity after successive reuse for five cycles. The TEM images and XRD patterns (Figure S13b-c) further demonstrated that there were no obvious changes in size and morphology after the durability tests.

In summary, we have developed a robust and tunable strategy for synthesizing porous multishell Au with in-situ surface modification based on controlling conversion of novel Au-melamine colloidal templates. Such a simple method is also suitable for generally fabricating Au-based bimetallic multishell structures. In $NH_3{\cdot}BH_3$-initiated hydrogenation of 4-nitrostyrene to 4-aminostyrene, the surface-modified Au displayed excellent selectivity in contrast with unmodified Au. Furthermore, porous multishell structures enabled Au sphere to display great increase of catalytic activity under irradiation of visible light. It is believed that our robust methods may provide new opportunities in constructing Au-based multishell materials with simple synthesis, controllable structure and enhanced performance.

Acknowledgements

The authors are grateful for the financial aid from the National Natural Science Foundation of China (21590794 and 21771173), the project development plan of science and technology of Jilin Province (20180101179JC), K. C. Wong Education Foundation (GJTD-2018-09), and CAS-CSIRO project (GJHZ1730).

Keywords: Multishell Au • Self-sacrificial templates • Plasmonic catalysis • Hydrogenation • Selectivity

[1] J. Li, S. Z. Jilani, H. Lin, X. Liu, K. Wei, Y. Jia, P. Zhang, M. Chi, Y. J. Tong, Z. Xi, S. Sun, *Angew. Chem., Int. Ed.* **2019**, *58*, 11527; *Angew. Chem.* **2019**, *131*, 10989.
[2] Z. Yin, Y. Wang, C. Song, L. Zheng, N. Ma, X. Liu, S. Li, L. Lin, M. Li, Y. Xu, W. Li, G. Hu, Z. Fang, D. Ma, *J. Am. Chem. Soc.* **2018**, *140*, 864.
[3] J. Bian, J. Feng, Z. Zhang, Z. Li, Y. Zhang, Y. Liu, S. Ali, Y. Qu, L. Bai, J. Xie, D. Tang, X. Li, F. Bai, J. Tang, L. Jing, *Angew. Chem., Int. Ed.* **2019**, *58*, 10873; *Angew. Chem.* **2019**, *131*, 11651.
[4] X. Zhao, L. Zhou, W. Zhang, C. Hu, L. Dai, L. Ren, B. Wu, G. Fu, N. Zheng, *Chem* **2018**, *4*, 1080.
[5] P. Liu, R. Qin, G. Fu, N. Zheng, *J. Am. Chem. Soc.,* **2017**, *139*, 2122.
[6] B. Wu, H. Huang, J. Yang, N. Zheng, G. Fu, *Angew. Chem., Int. Ed.* **2012**, *51*, 3440; *Angew. Chem.* **2012**, *121*, 3476.
[7] H. Lindlar, *Helv. Chim. Acta* **1952**, *35*, 446.
[8] Z. Chen, G. D. Q. Silveira, X. Ma, Y. Xie, Y. A. Wu, E. Barry, T. Rajh, H. C. Fry, P. D. Laible, E. A. Rozhkova, *Angew. Chem., Int. Ed.* **2019**, *58,* 4896; *Angew. Chem.* **2019**, *131,* 4950.
[9] H. Cheng, K. Fuku, Y. Kuwahara, K. Mori, H. Yamashita, *J. Mater. Chem. A* **2015**, *3*, 5244.
[10] Y. Wei, J. Wang, R. Yu, J. Wan, D. Wang, *Angew. Chem., Int. Ed.* **2019**, *58*, 1422; *Angew. Chem.* **2019**, *131*, 1436.
[11] M. Waqas, Y. Wei, D. Mao, J. Qi, Y. Yang, B. Wang, D. Wang, *Nano Res.* **2017**, *10*, 3920.
[12] Y. G. Sun, B. Wiley, Z. Y. Li, Y. N. Xia, *J. Am. Chem. Soc.* **2004**, *126*, 9399.
[13] X. Xia, Y. Wang, A. Ruditskiy, Y. Xia, *Adv. Mater.* **2013**, *25*, 6313.
[14] L.-L. Wu, Z. Wang, Y. Long, J. Li, Y. Liu, Q.-S. Wang, X. Wang, S.-Y. Song, X. Liu, H.-J. Zhang, *Small* **2017**, *13,* 1604272.
[15] X. Wang, L. Yu, B. Y. Guan, S. Song, X. W. Lou, *Adv. Mater.* **2018**, *30,* 1801211.
[16] X. Wang, J. Feng, Y. Bai, Q. Zhang, Y. Yin, *Chem. Rev.* **2016**, *116,* 10983.
[17] L. Zhou, Z. Zhuang, H. Zhao, M. Lin, D. Zhao, L. Mai, *Adv. Mater.* **2017**, *29,* 1602914.
[18] A. M. Spokoyny, D. Kim, A. Sumrein, C. A. Mirkin, *Chem. Soc. Rev.* **2009**, *38,* 1218.
[19] W. Lin, W. J. Rieter, K. M. L. Taylor, *Angew. Chem., Int. Ed.* **2009**, *48,* 650; *Angew. Chem.* **2009**, *121*, 660.
[20] B. Liu, H. Yao, W. Song, L. Jin, I. M. Mosa, J. F. Rusling, S. L. Suib, J. He, *J. Am. Chem. Soc.* **2016**, *138,* 4718.
[21] Z. Liu, J. Qi, M. Liu, S. Zhang, Q. Fan, H. Liu, K. Liu, H. Zheng, Y. Yin, C. Gao, *Angew. Chem., Int. Ed.* **2018**, *57,* 11678; *Angew. Chem.* **2018**, *130*, 11852.
[22] L. Zhang, H. B. Wu, X. W. Lou, *J. Am. Chem. Soc.* **2013**, *135,* 10664.
[23] Z. Teng, C. Wang, Y. Tang, W. Li, L. Bao, X. Zhang, X. Su, F. Zhang, J. Zhang, S. Wang, D. Zhao and G. Lu, *J. Am. Chem. Soc.* **2018**, *140,* 1385.
[24] Z. Teng, W. Li, Y. Tang, A. Elzatahry, G. Lu and D. Zhao, *Adv. Mater.* **2019**, *31*, e1707612.
[25] P. Serna, A. Corma, *ACS Catal.* **2015**, *5,* 7114.
[26] Y. Tan, X. Y. Liu, L. Zhang, A. Wang, L. Li, X. Pan, S. Miao, M. Haruta, H. Wei, H. Wang, F. Wang, X. Wang, T. Zhang, *Angew. Chem., Int. Ed.* **2017**, *56,* 2709; *Angew. Chem.* **2017**, *129*, 2753.
[27] F. Fu, C. Wang, Q. Wang, A. M. Martinez-Villacorta, A. Escobar, H. Chong, X. Wang, S. Moya, L. Salmon, E. Fouquet, J. Ruiz, D. Astruc, *J. Am. Chem. Soc.* **2018**, *140,* 10034.
[28] X. Yang, L. Zhao, T. Fox, Z.-X. Wang and H. Berke, *Angew. Chem., Int. Ed.* **2010**, *49*, 2058; *Angew. Chem.* **2010**, *122*, 2102.
[29] S. Rej, C. F. Hsia, T. Y. Chen, F. C. Lin, J. S. Huang, M. H. Huang, *Angew. Chem. Int., Ed.* **2016**, *55*, 7222; *Angew. Chem.* **2016**, *128*, 7338.
[30] E. Vasilikogiannaki, C. Gryparis, V. Kotzabasaki, I. N. Lykakis and M. Stratakis, *Adv. Synth. Catal.* **2013**, *355*, 907.
[31] Z. Huang and T. Autrey, *Energy Environ. Sci.* **2012**, *5*, 9257.
[32] M. Makosch, W.-I. Lin, V. Bumbalek, J. Sa, J. W. Medlin, K. Hungerbuehler, J. A. van Bokhoven, *ACS Catal.* **2012**, *2,* 2079.
[33] G. Hergert, J. Vogelsang, F. Schwarz, D. Wang, H. Kollmann, P. Gross, C. Lienau, E. Runge, P. Schaaf, *Light: Sci. Appl.* **2017**, *6*. e17075.
[34] J. Zhang, M. ElKabbash, R. Wei, S. C. Singh, B. Lam, C. Guo, *Light: Sci. Appl.* **2019**, *8*. DOI 10.1038/s41377-019-0164-8.
[35] A. G. M. da Silva, T. S. Rodrigues, V. G. Correia, T. V. Alves, R. S. Alves, R. A. Ando, F. R. Ornellas, J. Wang, L. H. Andrade, P. H. C. Camargo, *Angew. Chem., Int. Ed.* **2016**, *55,* 7111; *Angew. Chem.* **2016**, *128*, 7227.
[36] L. Jiang, T. Yin, A. M. Dubrovkin, Z. Dong, Y. Chen, W. Chen, J. K. W. Yang, Z. Shen, *Light: Sci. Appl.* **2019,** *8.* DOI 10.1038/s41377-019-0134-1.

COMMUNICATION

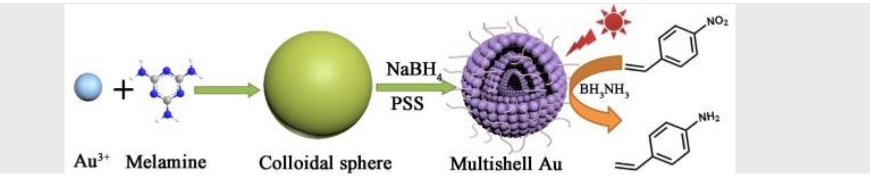

We report a robust self-template strategy for facile synthesis of Au-based multishell structure with controllable shell number, metal component and sphere size. In $NH_3 \cdot BH_3$-initiated hydrogenation of 4-nitrostyrene to 4-aminostyrene, the surface-modified multishell Au displays enhanced plasmonic catalysis activity and excellent selectivity.

Jian Li, Yan Long, Yu Liu, Lingling Zhang, Qishun Wang, Xiao Wang, Shuyan Song, and Hongjie Zhang*

Page No. – Page No.

Robust synthesis of Au-based multishell structures as plasmonic catalysts for selective hydrogenation of 4-nitrostyrene